Journal of ELECTRONIC MATERIALS, Vol. 39, No. 12, 2010
DOI: 10.1007/s11664-010-1370-6
© 2010 TMS

Impact Testing of Sn-3.0Ag-0.5Cu Solder with Ti/Ni(V)/Cu Under Bump Metallization After Aging at 150°C

KAI-JHENG WANG,[1] JENQ-GONG DUH,[1,4] BOB SYKES,[2] and DIRK SCHADE[3]

1.—Department of Materials Science and Engineering, National Tsing Hua University, Hsinchu, Taiwan. 2.—XYZTEC bv, Panningen, The Netherlands. 3.—XYZTEC bv, Günthersdorf, Germany. 4.—e-mail: jgd@mx.nthu.edu.tw

Nonmagnetic Ni(V) metal and low consumption rate with solders are the advantages of sputtered Ti/Ni(V)/Cu under bump metallization (UBM). However, a Sn-rich phase ("Sn-patch" herein) can form in the Ni(V) layer after reflow and aging. In lead-free solder, Sn-patches form and grow more quickly than in Sn-Pb solder. Thus, the effect of Sn-patches on solder joint reliability becomes critical. In this study, Sn-3.0Ag-0.5Cu solder was reflowed with Ti/Ni(V)/Cu UBM at 250°C for 60 s, and then aged at 150°C for various durations. A high-speed impact test was introduced to evaluate solder joint reliability. After impact testing, it was found that, the larger the Sn-patch, the greater the propensity of the solder joint to suffer brittle fracture. The correlation between Sn-patch and solder joint reliability is discussed.

Key words: High-speed impact test, Sn-patch, Ni(V) UBM

INTRODUCTION

Flip-chip technology has received considerable attention due to its advantages of higher input/output interconnect density and better electrical and thermal performance.[1,2] Under bump metallization (UBM) composed of multimetallic thin films is a critical part of flip-chip technology to improve solder joint reliability. Ti/Ni(V)/Cu UBM is popular in flip-chip technology due to the lower reaction rate with Sn and no magnetic influence during sputtering. However, a Sn-rich phase, the so-called Sn-patch, can grow into the Ni(V) layer during reflow and aging.[3–13] Recently, it was revealed that the Sn-patch consists of an amorphous Sn phase and crystalline V_2Sn_3, and a mechanism for its formation was proposed.[11] However, there is little literature concerning the relationship between Sn-patch and solder joint reliability. Zheng et al.[12] reported that the fracture surface of Sn-3.5Ag-1.0Cu solder joints with Ti/Ni(V)/Cu UBM became brittle after 30 reflows. Nevertheless, the shear force of solder joints was not decreased. A recent study by Wang and Duh[13] revealed that there was no decrease in the shear forces of Sn-3.0Ag-0.5Cu solder with Ti/Ni(V)/Cu UBM, and the fracture surface of solder joints was ductile after aging at 125°C for 2000 h. This implied that the formation of Sn-patch did not significantly affect solder joint reliability with Ni(V)-based UBM. In fact, the test speed in the previous studies was too low to evaluate the effect of Sn-patch on solder joint reliability. Based on the literature,[14,15] high-speed testing (i.e., at more than 10 mm/s) is a more effective method for the measurement of impact fracture strength in solder joints. Morita et al.[16] reported that the effect of Kirkendall voids on Sn-Ag-Cu/Cu solder joints was more evident with high-speed than low-speed testing. Therefore, in this study, the high-speed impact test was employed to evaluate the reliability of Sn-3.0Ag-0.5Cu solder joints with Ti/Ni(V)/Cu UBM, and the effect of Sn-patch on reliability is discussed.

(Received February 26, 2010; accepted August 16, 2010; published online September 14, 2010)

EXPERIMENTAL PROCEDURES

The thickness of Ti/Ni(V)/Cu UBMs was varied by controlling the sputtering time to achieve 0.5 μm,

1.0 μm, and 1.5 μm Cu layers. The thickness of Ti and Ni(V) was 0.1 μm and 2.0 μm, respectively. Ti/Ni(V)/Cu UBM with 0.5 μm, 1.0 μm, and 1.5 μm Cu layers are designated as UBM 05, UBM 10, and UBM 15, respectively. The 300-μm Sn-3.0Ag-0.5Cu solder ball was reflowed with Ti/Ni(V)/Cu UBM at 250°C for 60 s. The pad diameter was 200 μm. Finally, specimens were treated at 150°C for 250 h, 500 h, and 1000 h.

Cross-section samples were mounted with G2 resin, and then prepared by a cross-section polisher (SM-09011; JEOL, Japan) to avoid damage from the mechanical polishing process. Interfacial morphologies of intermetallic compounds (IMCs) were observed using a field-emission scanning electron microscope (FE-SEM, JSM-7600F; JEOL, Japan).

The high-speed impact test of solder joints was measured using a XYZTEC bonding tester with 115 gf pendulum (Condor 100; XYZTEC, The Netherlands). The impact height was 30 μm, and the impact speed was 100 mm/s. Ten aged solder joints were tested. The fracture surface of the solder joints was observed by FE-SEM with an energy-dispersive spectrometer (EDS; X-Max, Oxford, UK) after the impact test. To evaluate the bonding energy and failure mode of solder joints, the solder joint prepeak energy and total energy were measured during the high-speed impact test. In Fig. 1, the solder joint prepeak energy, which is correlated with the bonding energy, is defined as the energy before the maximal force. The solder joint total energy characterizes the failure mode. If the solder joint failure mode is ductile, the total energy is large, as shown in Fig. 1a. In contrast, the total energy of brittle fracture is small, as indicated in Fig. 1b.

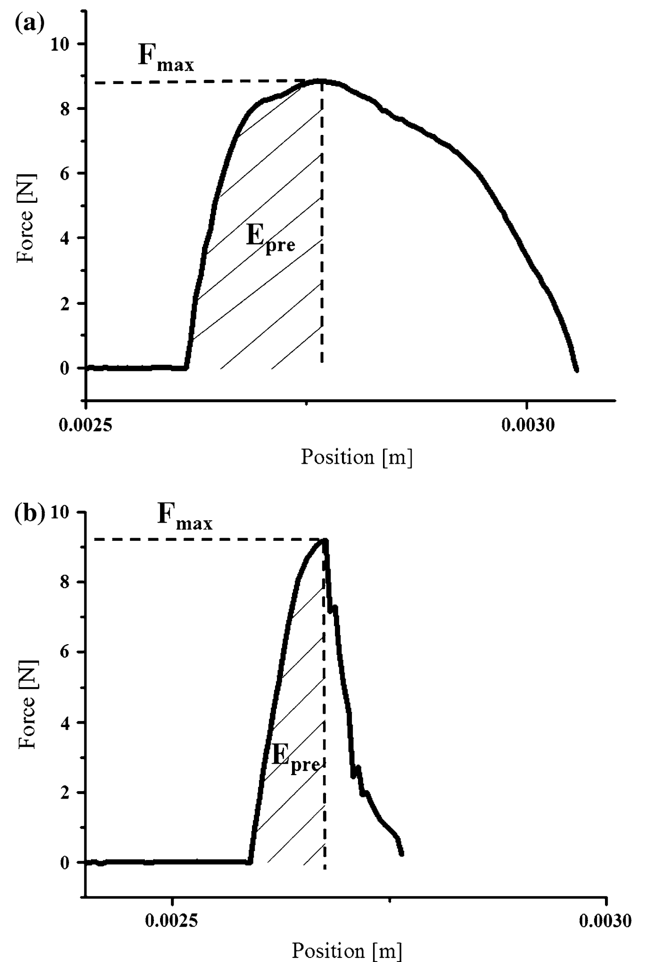

Fig. 1. Force versus position curve for (a) ductile and (b) brittle solder joint failure in a high-speed impact test.

RESULTS AND DISCUSSION

Figure 2 shows the microstructure of the Sn-3.0Ag-0.5Cu solder with Ti/Ni(V)/Cu UBM after various periods of isothermal aging. After reflow, the Cu layer of UBMs was all consumed, and Cu_6Sn_5 formed at the interface between the solder and Ni(V) layer. The Cu_6Sn_5 thickness in the Sn-Ag-Cu/UBM 05 solder joint is around 1.0 μm, and increases to 1.8 μm after aging at 150°C for 1000 h, as shown in Fig. 3a. The thickness of Cu_6Sn_5 was digitally measured by using Optimas software. The average thickness of the Cu_6Sn_5 layer was calculated by dividing the measured area of Cu_6Sn_5 by the length of the interface. Sn-patch was observed in the Ni(V) layer after reflow, in agreement with the literature report.[8–13] The area ratio of Sn-patch to the Ni(V) layer was around 13.2% in the Sn-Ag-Cu/UBM 05 solder joint after reflow, and increased to 14.1% after aging for 1000 h due to interdiffusion of Ni and Sn (Fig. 3b).

To evaluate the effect of Sn-patch on solder joint reliability, the high-speed impact test was employed. Figure 4 shows a box plot of solder joint prepeak energy and total energy after impact test. The bottom and top of the box define the lower and upper quartile, respectively. The band near the middle of the box indicates the median, and the square marker indicates the average energy of each condition. The whiskers show the minimum and maximum values. The prepeak energy of as-reflowed Sn-Ag-Cu/UBM 05 solder joints ranged between 0.005 mJ and 0.023 mJ (i.e., whiskers), and the average prepeak energy was 0.011 mJ (i.e., square marker), as shown in Fig. 4a. The average prepeak energy of Sn-Ag-Cu/UBM 05 solder joints after aging was around 0.010 mJ, identical to that before aging. The average total energy of the as-reflowed Sn-Ag-Cu/UBM 05 solder joint was 0.025 mJ, similar to the average prepeak energy, as shown in Fig. 4b. The total energy can be used to characterize the solder joint failure mode. As a result, if the total energy is similar to the prepeak energy, it is inferred that the failure mode is brittle, as indicated in Fig. 1b. In the high-speed impact test, the total energy of the Sn-Ag-Cu/UBM 05 solder joint after aging was similar to the as-reflowed ones, and the failure mode was totally brittle.

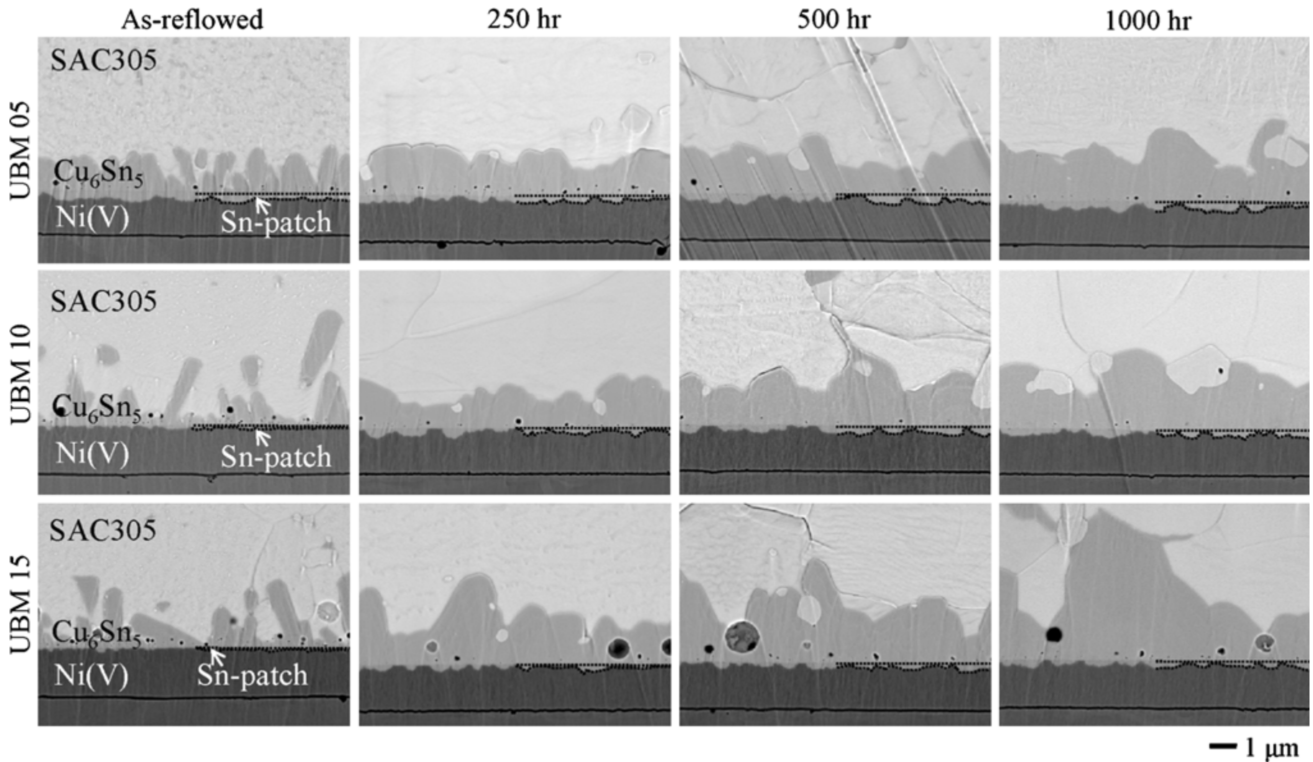

Fig. 2. Microstructures of Sn-Ag-Cu solder joints with Ti/Ni(V)/Cu UBM after aging at 150°C for various periods of time.

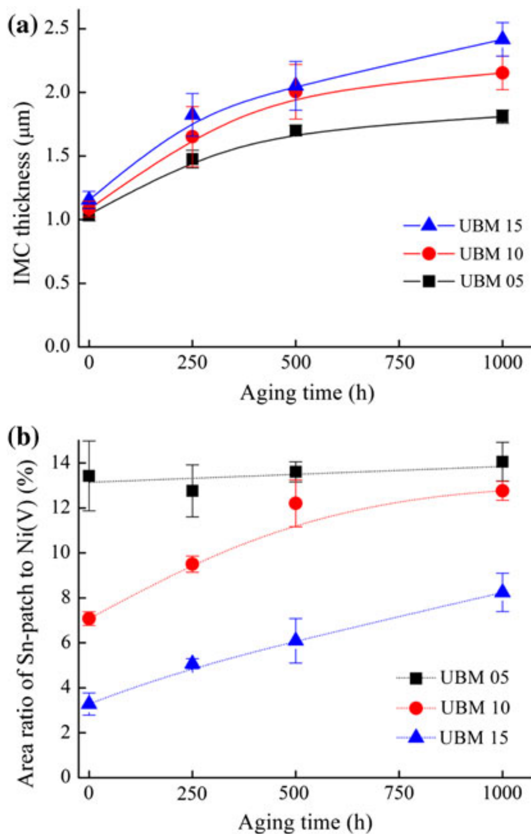

Fig. 3. (a) IMC thickness and (b) area ratio of Sn-patch to Ni(V) of Sn-Ag-Cu solder joints with Ti/Ni(V)/Cu UBM after aging at 150°C for various periods of time.

When the thickness of the Cu layer was increased to 1.0 μm (i.e., UBM 10), Cu_6Sn_5 was 1.2 μm thick (Fig. 3a) after reflow and increased to 2.2 μm after aging for 1000 h. The area percentage of Sn-patch was 7.1% after reflow (Fig. 3b). The data show that the thicker Cu layer in the Sn-Ag-Cu/UBM 10 solder joint supplied more Cu to form thicker Cu_6Sn_5. In addition, Cu_6Sn_5 acted as a diffusion barrier which slowed Ni diffusion. As a result, the area ratio of Sn-patch to Ni(V) layer was decreased in the Sn-Ag-Cu/UBM 10 solder joint after reflow. The area percentage of Sn-patch increased to 12.7% after aging for 1000 h, which was also smaller than that in the Sn-Ag-Cu/UBM 05 solder joint.

The average prepeak energy of the Sn-Ag-Cu/UBM 10 solder joint was 0.012 mJ before aging and increased to 0.028 mJ after aging for 250 h (Fig. 4a). The average total energy of the Sn-Ag-Cu/UBM 10 solder joint increased from 0.031 mJ to 0.061 mJ after aging for 250 h, as shown in Fig. 4b. It was inferred that the failure mode was a mix of brittle and ductile, so both prepeak energy and total energy increased after aging for 250 h. In addition, from Fig. 4, the maxima of both prepeak energy and total energy in Sn-Ag-Cu/UBM 10 solder joints before and after aging were much higher than for Sn-Ag-Cu/UBM 05. However, after aging for 500 h, both prepeak energy and total energy decreased and the failure mode became more brittle. In comparison with the Sn-Ag-Cu/UBM 05 solder joint, the Cu_6Sn_5 formed in the Sn-Ag-Cu/UBM 10 solder joint was thicker. In fact, the IMC at the solder joint interface

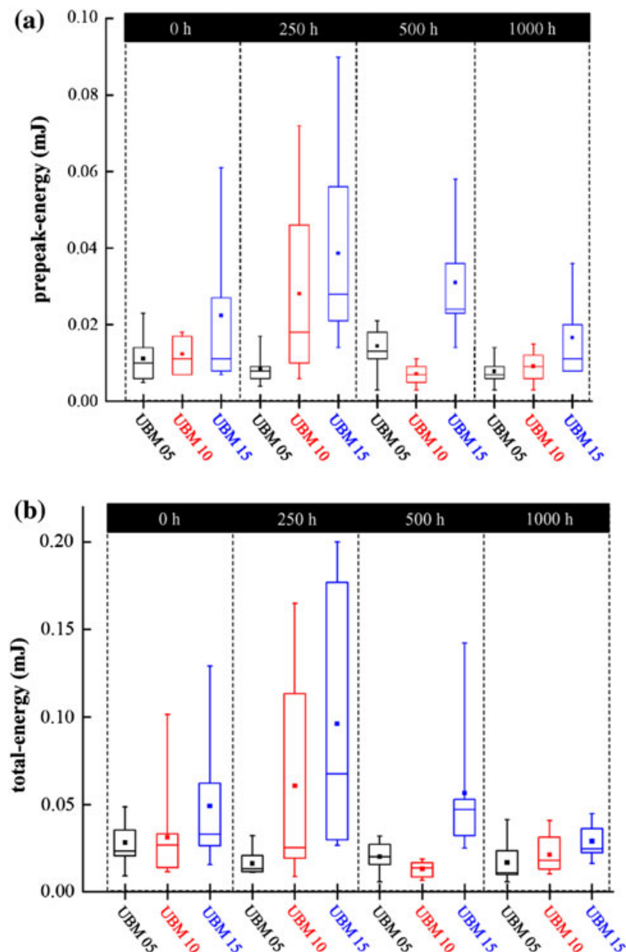

Fig. 4. Box plot of (a) prepeak energy and (b) total energy of Sn-Ag-Cu solder joints with Ti/Ni(V)/Cu UBM after aging at 150°C for various periods of time.

played an interlocking role between the solder and UBM. However, if the IMC was too thick, this would reduce the bonding energy of the solder joint due to the brittleness of the IMC. In the Sn-Ag-Cu/UBM 05 solder joint, the thickness of Cu_6Sn_5 was smaller than that in the Sn-Ag-Cu/UBM 10 solder joint. However, the bonding energy of the Sn-Ag-Cu/UBM 05 solder joint was lower than that of the Sn-Ag-Cu/UBM 10 solder joint. Therefore, the thickness of the IMC may not be the sole factor in the reliability of Sn-Ag-Cu solder with Ti/Ni(V)/Cu solder joint.

To determine the critical factor in the reliability of Sn-Ag-Cu solder with Ti/Ni(V)/Cu UBM, the Cu layer of UBM was increased to 1.5 μm (i.e., UBM 15) to form thicker Cu_6Sn_5 at the solder joint interface along with less Sn-patch. The Cu_6Sn_5 was 1.2 μm after reflow, which was thicker than that of Sn-Ag-Cu/UBM 05 and Sn-Ag-Cu/UBM 10 solder joints. Cu_6Sn_5 at the interface between Sn-Ag-Cu solder and UBM 15 grew to 2.4 μm after aging for 1000 h (Figs. 2 and 3a). The area percentage of Sn-patch in the Sn-Ag-Cu/UBM 15 solder joint was 3.3% before aging and increased to 8% after aging for 1000 h (Figs. 2 and 3b). In the high-speed impact test, both the prepeak energy and total energy of Sn-Ag-Cu/UBM 15 solder joints were much higher than those of the Sn-Ag-Cu/UBM 05 and Sn-Ag-Cu/UBM 10 solder joints after reflow and aging (Fig. 4a). From FE-SEM images, such as those shown in Fig. 5, the failure mode of the Sn-Ag-Cu/UBM 15 solder joint was near ductile after reflow and aging for 250 h, but became totally brittle after aging for 1000 h. The data in Fig. 4b show that, if the average total energy was below 0.05 mJ, the solder joint failure mode was totally brittle. In contrast, the failure mode tended to be more ductile if the total energy was higher than 0.05 mJ. It should be noted that the solder joint was broken without ductile deformation during the impact test. As a result, the solder joint total energy was similar to its prepeak energy (Fig. 4).

Figure 3a reveals that the Cu_6Sn_5 thickness is around 1.9 μm in both the Sn-Ag-Cu/UBM 10 solder joints aged for 500 h and the Sn-Ag-Cu/UBM 15 solder joints aged for 250 h. However, the failure mode was different in these solder joints. In the Sn-Ag-Cu/UBM 10 solder joints aged for 500 h, the failure mode was totally brittle. In contrast, both ductile and brittle failure were observed for the Sn-Ag-Cu/UBM 15 solder joints aged for 250 h. This implies that the IMC thickness was not the only factor affecting the reliability of solder joint with Ti/Ni(V)/Cu UBM.

Figure 5 shows FE-SEM images of the fracture surface, indicating that ductile solder joint failure occurred inside the solder (Fig. 5a). Figure 5b shows solder joint brittle failure, indicating that some IMC was exposed on the surface. To evaluate where the fracture interface was, x-ray mapping was employed, as shown in Fig. 5c. There were Cu- and Sn-rich regions on the right-hand side of image, which was also confirmed by EDS as Cu_6Sn_5 IMC. The left-hand side of the image (Fig. 5c) was rich in Ni and V, indicating the Ni(V) layer. Sn concentrated in some areas in the Ni(V) layer, which was the so-called Sn-patch. It was inferred that the interface between Sn-patch and IMC was weak, and so the fracture occurred at this interface. Chen and Chen reported that the Sn-patch phase was a dewetting layer for IMC, which was easily spalled into the solder after reflow at 250°C for 6 h.[15]

This phenomenon was similar to the case of the Ni-Sn-P phase in the solder joint with electroless Ni-P layer. Lin et al.[17,18] reported that the Ni-Sn-P phase formed at the interface between Sn-Ag-Cu solder and high-P Ni-P layer after one reflow, and the IMC was easily detached from Ni-Sn-P after multiple reflows. Solder joint reliability decreased when the Ni-Sn-P phase formed.[19] In this study, the Sn-patch acted as the dewetting layer formed in the Ni(V) layer, reducing the bonding energy of the Sn-Ag-Cu solder joint with Ti/Ni(V)/Cu UBM. The fracture surface of all solder joints became brittle when aged for 1000 h (Fig. 4b). Compared

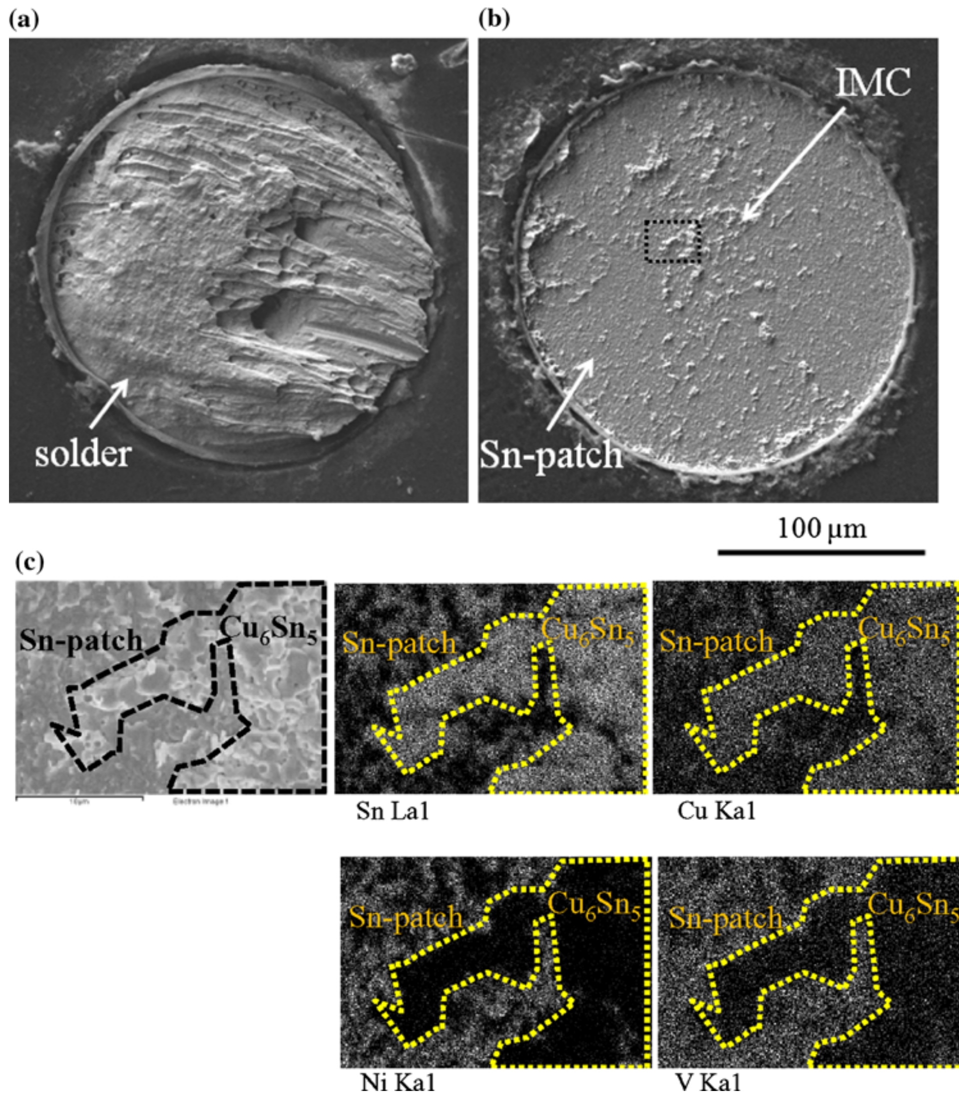

Fig. 5. FE-SEM images of (a) ductile and (b) brittle fracture surfaces of Sn-Ag-Cu solder joints with UBM 15, and (c) x-ray mapping of the magnified image marked in (b) after aging at 150°C for 250 h.

with the area percentage of Sn-patch (Fig. 3b), it was revealed that, if the area ratio of Sn-patch to Ni(V) layer was around 8% (i.e., Sn-Ag-Cu/UBM 15 solder joint aged for 1000 h), solder joint brittle fracture was observed, and the bonding energy of the solder joint was weak.

In this study, the relationship between Sn-patch and the reliability of Sn-Ag-Cu solder with Ti/Ni(V)/Cu UBM was probed. Both IMC thickness and Sn-patch area affected solder joint reliability. This work demonstrates that the effect of Sn-patch on solder joint reliability was more significant than that of IMC thickness.

CONCLUSIONS

Both Cu_6Sn_5 and Sn-patch formed at the interface of a Sn-Ag-Cu solder joint with Ti/Ni(V)/Cu UBM after reflow, and grew with aging time. IMC thickness was not the most important factor in solder joint reliability. Sn-patch formation affected reliability when the area ratio of Sn-patch to Ni(V) layer exceeded 8%, the bonding energy decreased significantly, and the failure mode became brittle.

ACKNOWLEDGEMENT

Financial support from the National Science Council, Taiwan, under Contract No. NSC-97-2221-E-007-021-MY3 and technical support from the XYZTEC Company, The Netherlands, are acknowledged.

REFERENCES

1. P.A. Totta and R.P. Sopher, *IBM J. Res. Dev.* 13, 226 (1969).
2. J.H. Lau, *Flip Chip Technologies* (New York: McGraw-Hill, 1996), p. 123.
3. C.H. Tung, P.S. Teo, and C. Lee, *IEEE Trans. Dev. Mater. Reliab.* 5, 212 (2005).
4. M. Li, F. Zhang, W.T. Chen, K. Zeng, K.N. Tu, H. Balkan, and P. Elenius, *J. Mater. Res.* 17, 1612 (2002).
5. F. Zhang, M. Li, C.C. Chum, and K.N. Tu, *J. Mater. Res.* 17, 2757 (2002).

6. F. Zhang, M. Li, C.C. Chum, and C.-H. Tung, *J. Mater. Res.* 18, 1333 (2003).
7. C.Y. Liu, K.N. Tu, T.T. Sheng, C.H. Tung, D.R. Frear, and P. Elenius, *J. Appl. Phys.* 87, 750 (2000).
8. A.T. Wu and F. Hua, *J. Mater. Res.* 22, 735 (2007).
9. G.Y. Jang, J.G. Duh, H. Takahashi, S.W. Lu, and J.C. Chen, *J. Electron. Mater.* 35, 1745 (2006).
10. G.Y. Jang and J.G. Duh, *J. Electron. Mater.* 35, 2061 (2006).
11. K.J. Wang, Y.Z. Tsai, J.G. Duh, and T.Y. Shih, *J. Mater. Res.* 24, 2638 (2009).
12. F. Zhang, M. Li, B. Balakrisnan, and W.T. Chen, *J. Electron. Mater.* 31, 1256 (2002).
13. K.J. Wang and J.G. Duh, *J. Electron. Mater.* 38, 2534 (2009).
14. F. Song, S.W.R. Lee, K. Newman, B. Sykes, and S. Clark, *Electronic Components and Technology Conference* (2007), p. 364.
15. S.W. Chen and C.C. Chen, *J. Electron. Mater.* 36, 1121 (2007).
16. T. Morita, R. Kajiwara, I. Ueno, and S. Okabe, *Jpn. J. Appl. Phys.* 47, 6566 (2008).
17. Y.C. Lin, T.Y. Shih, S.K. Tien, and J.G. Duh, *J. Electron. Mater.* 36, 1469 (2007).
18. Y.C. Lin, T.Y. Shih, S.K. Tien, and J.G. Duh, *Scripta Mater.* 56, 49 (2007).
19. Y.C. Sohn, J. Yu, S.K. Kang, D.Y. Shih, and T.Y. Lee, *J. Mater. Res.* 19, 2428 (2004).